Unusual Phase Behavior of a Mesogen-Jacketed Liquid Crystalline Polymer Synthesized by Atom Transfer Radical Polymerization

Yong-Feng Zhao,[†] Xing-He Fan,*[,†] Xin-Hua Wan,[†] Xiao-Fang Chen,[†] Yi Yi,[†] Liang-Shi Wang,[‡] Xia Dong,[§] and Qi-Feng Zhou*[,†]

Department of Polymer Science and Engineering, College of Chemistry and Molecular Engineering, Peking University, Beijing 100871, China; Key Laboratory of Polymer Chemistry and Physics, Ministry of Education, Beijing 100871, China; Beijing Research Institute of Chemical Industry, China Petroleum and Chemical Corporation, Beijing 100013, China; and State Key Laboratory of Polymer Physics and Chemistry, Joint Laboratory of Polymer Science and Materials, Institute of Chemistry, Chinese Academy of Sciences, Beijing 100080, China

Received July 3, 2005; Revised Manuscript Received November 3, 2005

ABSTRACT: A series of mesogen-jacketed liquid crystalline polymers, poly{2,5-bis[(4-butoxyphenyl)oxycarbonyl]-styrenes} (PBPCS), with a wide range of molecular weights ($M_n = 1.24 \times 10^4 - 35.6 \times 10^4$) and narrow molecular weight distributions ($M_w/M_n \leq 1.18$) have been synthesized by atom transfer radical polymerization. The resulting polymers have been investigated by a combination of techniques including differential scanning calorimetry, polarized optical microscopy, and X-ray scattering. The samples with $M_n \leq 2.42 \times 10^4$ are isotropic. The samples with $M_n \geq 3.36 \times 10^4$ display a thermodynamically stable isotropic phase at lower temperature and a liquid crystalline (LC) phase at higher temperature. The phase behavior shows a phenomenon quite similar to the reentrant isotropic phase. These transitions are correlated with the rheological properties measured as a function of temperature. The rheological behavior of the polymer in the isotropic phase and in the LC phase has been studied as well. On the basis of these experimental observations, a generalized phase diagram is constructed for the polymers showing the influence of the molecular weight on the phase transition temperature. It is illustrated that LC phase is formed through a global change of the whole molecule from the coiled to extended chain conformation accompanied by an increase of the entropy. Higher entropy originating from the free mobilities of bulky side chains in LC phase has been proposed to be an important factor to stabilize the LC phase.

Introduction

There are two major classes of thermotropic liquid crystalline (LC) polymers, main-chain LC polymers and side-chain LC polymers, according to the position of the mesogenic groups in the polymers.[1] For main-chain LC polymers, the mesogenic groups are parts of polymer main chain, and the resulting polymers are relatively rigid. For side-chain LC polymers, the mesogenic groups can either terminally or laterally attach to polymer backbone. To decouple the interaction between backbone and mesogenic groups in side chain, flexible spacers are usually introduced to side-chain LC polymers.[2] In such a condition, the mesogenic side group can be anisotropically ordered to form LC phase even though the backbone tends to adopt the statistical random coil conformation.

Another type of LC polymer called "mesogen-jacketed liquid crystalline polymers" (MJLCPs) is proposed when the mesogenic groups are attached laterally to the backbone through their center of gravity with short or no spacers.[3,4] Unlike the conventional side-chain LC polymers whose backbones usually take a random-coil chain conformation, MJLCPs are somewhat rigid and exhibit some features of main-chain LC polymers because of the strong interaction between the main chain and high population of bulky side groups. The specific characteristic of MJLCPs is that the director of the LC phase is determined by the main chain instead of the side chain. Following the concept, we have synthesized such kinds of polymers that exhibit LC behavior though the side chains do not have mesogenic side groups, like poly{di(cyclohexyl)vinyl terephthalate}[5] and poly-{di(4-heptyl)vinyl terephthalate}.[6] The steric hindrance effects among the side groups and the interaction between the side group and the main chain have been suggested to play a critical role in the formation of LC phase. In addition, the LC phase is even observed in a series of poly{di(alkyl)vinylterephalated} (PDAVTs) with linear alkyl groups incorporated into the pendant groups of PDAVTs.[7] The effect of the side-group size on the phase structure has been described. In this respect, MJLCPs are similar to flexible polymer poly(dialkylsiloxanes) and poly-(di-*n*-alkoxyphosphazenes) exhibiting a mesomorphic state with no mesogens.[8−11] The LC phase structures of MJLCPs are identified as columnar nematic phase,[12] hexagonal columnar nematic phase,[13] and hexagonal columnar LC phase[6,7] in which each cylinder is formed by a single MJLCPs chain molecule.[13]

Recently, we have observed that the LC phase of some MJLCPs does not appear immediately above glass transition, and the intensity of WAXD decreased on the cooling.[13−15] On the more detailed studies, we have synthesized a series of poly-{2,5-bis[(4-butoxyphenyl)oxycarbonyl]styrene}, PBPCS, with different molecular weights by atom transfer radical polymerization (ATRP) and studied its phase transitions depending on the molecular weight. The results show an unusual fact that some PBPCS get into an isotropic phase at lower temperature and then form a LC phase. This observation may provide useful information for the origin of LC phase in MJLCPs and the polymers exhibiting mesomorphic state with no mesogens.

Experimental Section

Materials. Chlorobenzene was purified by washing with concentrated sulfuric acid to remove thiophene, followed by washing

[†] Peking University.
[‡] China Petroleum and Chemical Corporation.
[§] Institute of Chemistry, CAS.
* Corresponding authors. E-mail: fanxh@pku.edu.cn or qfzhou@pku.edu.cn.

10.1021/ma0514370 CCC: $33.50
Published on Web 01/06/2006

Scheme 1. Chemical Structure and Synthesis of PBPCS

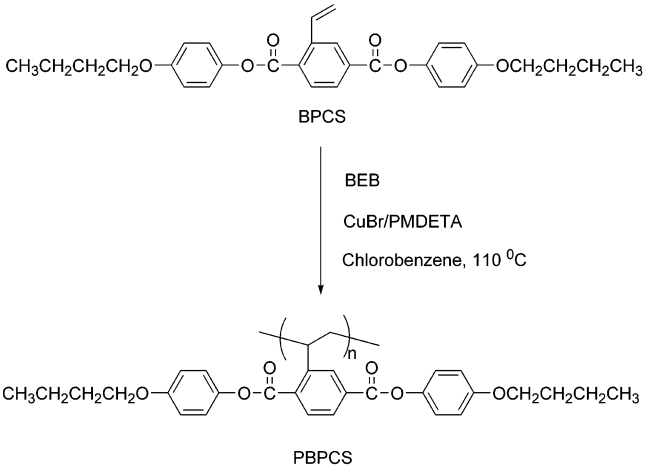

with water, and then dried and distilled. Cuprous bromide (CuBr) was synthesized from $CuBr_2$ and purified by stirring in acetic acid and washing with methanol and then dried in a vacuum just before use. *N*,*N*,*N*′,*N*″,*N*″-Pentamethyldiethylenetriamine (PMDETA) (99.5%, TCI) and 1-bromoethylbenzene (BEB) (97%, Acros) were used as received without further purification.

Synthesis of Monomer and Polymers. The chemical structure and synthesis of the polymer are shown in Scheme 1. BPCS was synthesized according to the literature.[14] The polymers were synthesized by atom transfer radical polymerization. Typically, CuBr (0.25 mg, 0.0017 mmol) and BPCS (0.5 g, 1.02 mmol) were placed into a 10 mL reaction tube containing a magnetic stir bar. Then, 10 μL of chlorobenzene solution of PMDETA (0.0017 mmol) and BEB (0.0017 mmol) was introduced with a syringe. After being added 1.3 g of chlorobenzene, the reaction mixture was purged with nitrogen and subjected to four freeze−thaw cycles to remove any dissolved oxygen and sealed under vacuum. The tube was place into an oil bath preset at 110 °C. After the polymerization was terminated by putting the tube into ice/water mixture, the tube was broken. The product was diluted with THF and passed through a basic alumina column to remove copper complex. The polymer was precipitated into methanol. Monomer conversion was determined by gravimetry.

Measurements. Gel permeation chromatography (GPC) measurements were carried out in THF on a Waters 2410 instrument equipped with three Waters μ-Styragel columns (10^3, 10^4, and 10^5 Å) at 35 °C, with a Waters 2410 RI detector. Calibration was based on polystyrene standards.

The thermogravimetric analysis (TGA) was performed on a TA SDT 2960 instrument at heating rate of 10 °C/min in a nitrogen atmosphere. DSC measurements were made on a Thermal Analysis Co. Q-100 instrument with Universal Analysis software under a dynamic atmosphere of N_2.

Polarized optical microscopy (POM) observation was conducted on a Leitz Laborlux 12 microscope with a Leitz 350 hot stage.

1D WAXD powder experiments were performed on a Philips X'Pert Pro diffractometer with a 3 kW ceramic tube as the X-ray source (Cu Kα) and an X'celerator detector. The sample stage was set horizontally. The reflection peak positions were calibrated with silicon powder ($2\theta > 15°$) and silver behenate ($2\theta < 10°$). Background scattering was recorded and subtracted from the sample patterns.

2D WAXD fiber pattern was obtained using Bruker D8Discover diffractometer with GADDS as a 2D detector. Again, the calibration was conducted using silicon powder and silver behenate. The sample was mounted on the sample stage, and the point-focused X-ray beam was aligned both perpendicular and parallel to the mechanical shearing direction. The 2D diffraction patterns were recorded in a transmission mode at room temperature. The oriented samples were prepared by mechanically shearing the films in the LC phase.

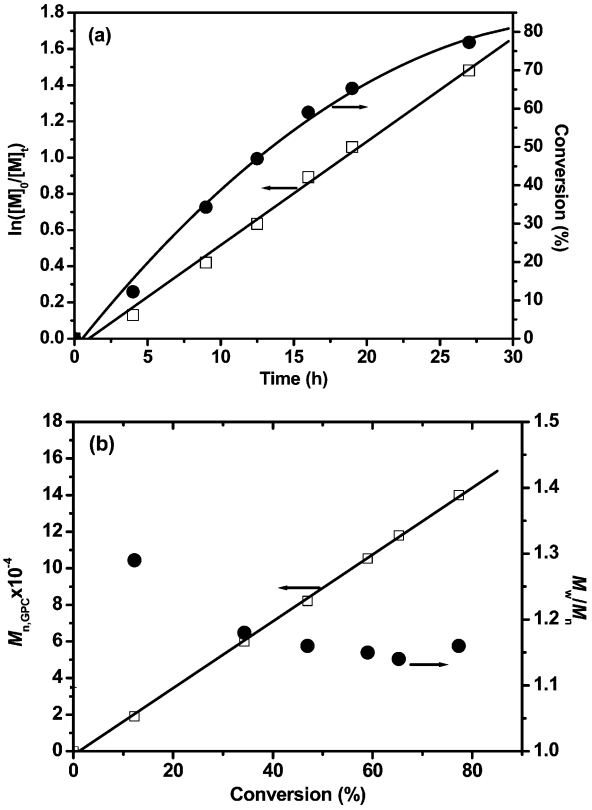

Figure 1. Relationships of the conversion and $\ln([M]_0/[M]_t)$ with the polymerization time for BPCS polymerization in chlorobenzene at 110 °C (a). Dependence of molecular weight and molecular weight distribution on the conversion of BPCS in chlorobenzene (b). The concentration is 40% (w/w).

A Rheometrics ARES rheometer was applied to measure the viscoelastic properties of the PBPCS based on oscillatory shear. The experimental temperature was controlled using forced N_2 gas convection. Isochronal temperature scans were carried out using a 25 mm diameter parallel-plate geometry with a frequency of 5 rad/s and a small strain amplitude. Isothermal frequency sweeps were made using the same setup at frequencies from 0.1 to 100 rad/s. The disk sample was prepared by solvent-casting from toluene in the present of an antioxidant, 2,6-di-*tert*-butyl-4-methylphenol (BHT), and then slowly evaporating the majority of the solvent first at room temperature for 1 week and then at 80 °C overnight in a vacuum oven to remove any residual solvent.

Results and Discussion

Synthesis of High Molecular Weight Polymers. High molecular weight polymers with controlled architecture are desirable for science and applications.[16] In our previous work, ATRP has been used to synthesize MJLCP with narrow molecular weight distribution using sparteine as the ligand, but the molecular weights are relatively low ($M_{n,GPC} < 20\,000$).[17] In this study, we used PMDETA as ligand with BEB as initiator to prepare PBPCS. Figure 1a shows the time dependence of $\ln([M]_0/[M]_t)$ and the conversion. Each data point represents a single experiment. The linear behavior of $\ln([M]_0/[M]_t)$ is consistent with a controlled polymerization that is first order in monomer concentration. The plots of molecular weight and molecular weight distribution vs conversion are illustrated in Figure 1b. The M_n valued by GPC is found to increase in direct proportion to the monomer conversion. It is revealed that the polymerization system is under good control in synthesizing high molecular weight PBPCS.

Table 1 summarizes the molecular characteristics for PBPCS with different molecular weight. In general, the molecular weight

Table 1. Molecular Characteristics and the Phase Transition Temperatures of PBPCS

sample	$M_n \times 10^{-4}$ [a]	M_w/M_n [a]	T_g (°C) [b]	T_x (°C) [b]	ΔH_x (kJ/mol) [b]
P-1	1.27	1.16	97.8		
P-2	2.42	1.16	104.3		
P-3	3.36	1.15	102.9	274[c]	
P-4	4.05	1.11	103.6	249[c]	
P-5	5.55	1.12	103.5	236.7	0.140
P-6	9.39	1.18	103.6	206.7	0.346
P-7	14.7	1.13	104.1	200.0	0.488
P-8	18.8	1.17	108.8	197.6	0.506
P-9	24.2	1.17	107.5	192.7	0.529
P-10	28.8	1.18	108.7	191.0	0.512
P-11	35.6	1.13	107.2	187.8	0.493

[a] Obtained from GPC, PS as standards. [b] Evaluated by DSC during second heating cycle at a rate of 10 °C/min. [c] Determined by POM during heating run at a rate of 10 °C/min.

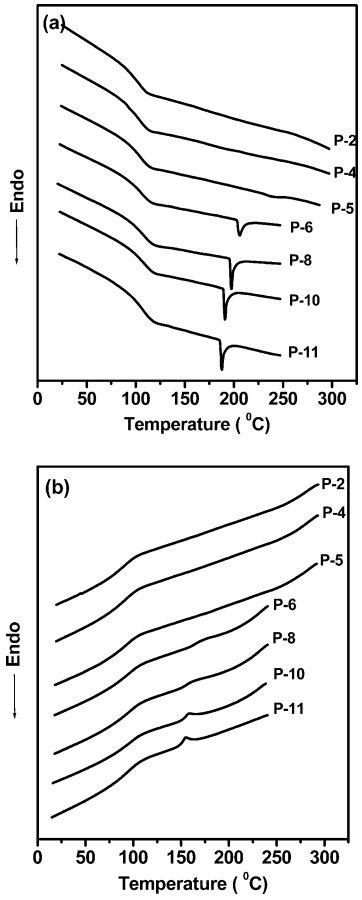

Figure 2. DSC curves of selected polymers during second heating scan (a) and first cooling scan (b) at a rate of 10 °C/min under a N_2 atmosphere.

distribution increase rapidly in a high molecular weight system because the slow termination process is not negligible in such a system with low initiator concentrations.[18,19] It is observed that PBPCS with very high molecular weights of (M_n = 350 000) still has low molecular weight distribution (less than 1.2).

Phase Transition and the Influence of the Molecular Weight. Figure 2a presents DSC curves for selected polymers during the second heating cycle at a rate of 10 °C/min. Besides the glass transition, a distinct first-order transition peak (noted as T_x) is observed when the molecular weights of the PBPCS are higher than 4.05×10^4. The values of transition temperatures for all samples are listed in Table 1. On the cooling curves (Figure 2b), corresponding exothermic peaks are observed at

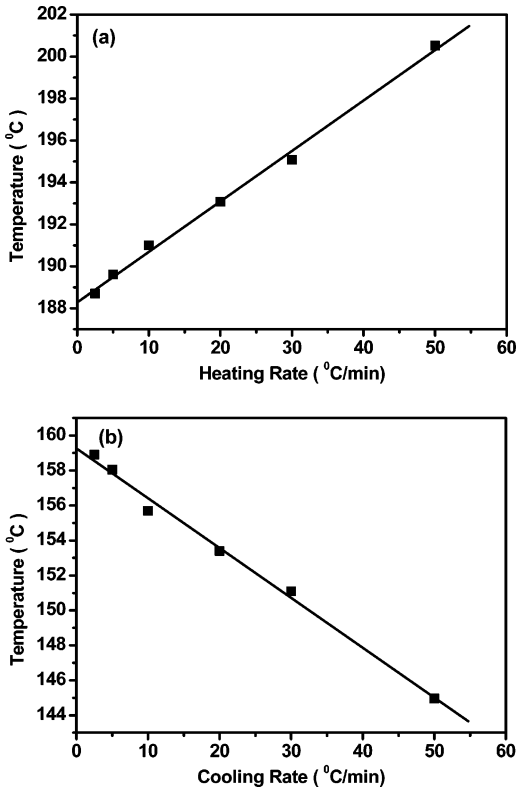

Figure 3. Plots of T_x with respect to the heating rates (a) and cooling rates (b) for sample P-10.

lower temperatures compared to the endothermic peaks. As an example for P-10, the endothermic peak is found at 191 °C, while the exothermic peak temperature of 156 °C is observed. The procedures can be reproduced several times, indicating a reversible phase transition occurred.

An interesting observation of DSC curves is that the heats of transition of endothermic process are identical and small (Table 1). This enthalpy is not only lower than the usual transition enthalpy of the crystallization and melting but also lower than the typical transition enthalpy of a nematic or smectic phase to isotropic phase transition.[20,21] It may imply that if this thermal event is associated with a certain transition, this transition must correlate with a small change of molecular interactions (an entropy term), which can be detected by DSC.

We also find that the transition temperatures are both heating and cooling rate dependent. Figure 3 exhibits the transition temperatures at different heating and cooling rates for sample P-10. The transition temperature increases with an increase of the heating rate, while its enthalpy does not change much. During cooling, the transition temperatures decrease with an increase of the cooling rate. Such a supercooling dependence of transition may represent a relaxation hysteresis during the supramolecular structure formation and disappearance which relates to a cooperative dynamics of the polymer chains.[6]

Polarized optical microscopy (POM) investigation of samples shows that there is birefringence at the above-mentioned transition temperatures. Figure 4 shows the observation for sample P-10. Upon heating, the sample becomes soft above the T_g, but there is no birefringence (Figure 4a). The LC texture is formed only when the temperature reaches about 191 °C (Figure 4b) at which a corresponding endotherm appears in DSC curve. Upon heating further, no visible change of birefringence is observed before decomposition (onset temperature > 300 °C). On the subsequent cooling the original scene is reestablished; i.e., the birefringence disappears (Figure 4c). This suggests that

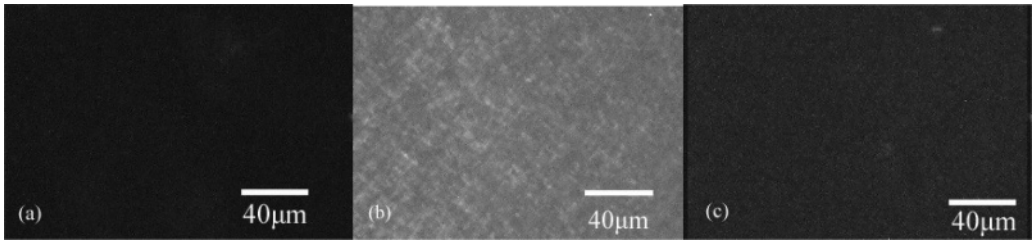

Figure 4. Polarized optical micrographs of sample P-10 at 170 (a), 210 (b), and 150 °C (c).

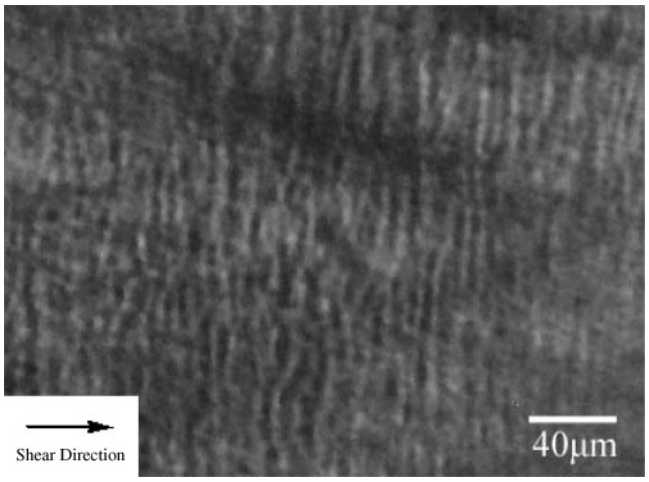

Figure 5. Banded texture of sample P-10 sheared at 210 °C.

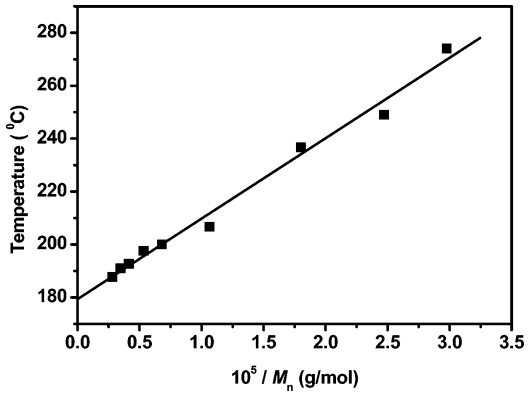

Figure 6. Plot of the transition temperature (T_x) against the reciprocal molecular weight.

the phase transition of the DSC curve corresponds to an isotropic−LC transition. The LC phase has been destroyed during the process of the cooling. It must be noticed that birefringence is observed at high temperature for the samples P-3 and P-4 (Table 1) though there is no endotherm at DSC curves. This may be ascribed to too small thermal heat to be detected by DSC for these two samples. For the samples with $M_n \leq 2.42 \times 10^4$ (P-1 and P-2), they become soft and flow when the samples are heated above 120 °C. On the continuous heating procedure, both samples maintain zero birefringence until over 300 °C. During cooling no birefringence is observed also.

When sample P-10 was mechanically sheared at 210 °C, bands with alternating birefringence can be formed, and the band spacing is between 4 and 5 μm (Figure 5). The normal to the direction of the band is parallel to the shear direction. This shear-induced LC banded texture is recognized as the important characterization of LC polymers. It is commonly understood that the banded texture can be formed only in low ordered LC phases and two-dimensional columnar phase. Highly ordered smectic and smectic crystal phase are solidlike and cannot be mechanically sheared to form these bands.[6] The same morphology has been observed for other MJLCPs with a rigid type of main chain.[13,22]

A detailed consideration of the phase transition shows that the phase transition temperatures of both the endothermic and the exothermic process depend on the molecular weights of samples. As shown in Figure 6, a plot of this transition temperature (T_x) against the reciprocal molecular weight indicates a linear relationship. The data for sample P-3 and P-4 obtained by POM are included as well. A large molecular weight dependence of the isotropization was reported in the system of the poly(diethylsiloxane) in which the mesophase−isotropic transition temperature increases with an increase of the molecular weight.[23] As a result, the heating rate dependence of phase transition and a linear relationship between phase transition temperature and reciprocal molecular weight are ascribed to the existence of extended chain conformation of the macromolecules in the mesophase. It is worthy to note that the phase transition temperature exhibits an unusual transition behavior for this work: the transition temperature decreases with an increasing of the M_n (Table 1). But the LC phase is more stable with an increasing of molecular weight for both systems.

LC Phase Identification of PBPCS. To confirm the phase transition which was indicated by optical and DSC investigation, 1D WAXD was conducted. Parts a and b of Figure 7 illustrate the two sets of 1D WAXD patterns of the as-cast sample (P-10) in the low 2θ (between 3° and 10°) angle regions obtained during the first heating and the first cooling at a rate of 5 °C/min. Below 185 °C, the low-angle diffraction peak is diffuse and weak. At temperatures above 185 °C, a sharp and intense peak at $2\theta = 4.75°$ (d spacing of 1.86 nm) appears at higher 2θ angle. With the further increasing temperature, the intensity of the peak increases rapidly. This peak becomes weak and disappears at 160 °C on the following cooling scan. The distinct discontinuous intensities correspond with the endothermal transition of DSC at about 190 °C during the second heating and the exothermal transition on cooling at about 156 °C. The discontinuous observation during cooling procedure clearly shows that the LC phase formed at higher temperature disappears during cooling. In parts c and d of Figure 7, the WAXD experiment reveals that the amorphous halo at the higher 2θ range retains the same shape. Upon heating, the center of halo is found to shift to lower 2θ in the beginning, followed by a shift to higher 2θ above glass transition, and then the halo shifts to lower 2θ at the temperature corresponding to the formation of the LC phase. The similar features are observed during the cooling scan.

In analogy to sample P-10, discontinuous scattering halos were observed by WAXD for samples P-4 and P-3. As shown in Figure 8, a sharp and intense peak at $2\theta = 4.74°$ (d spacing of 1.86 nm) appears at the temperature above 245 °C for P-4.

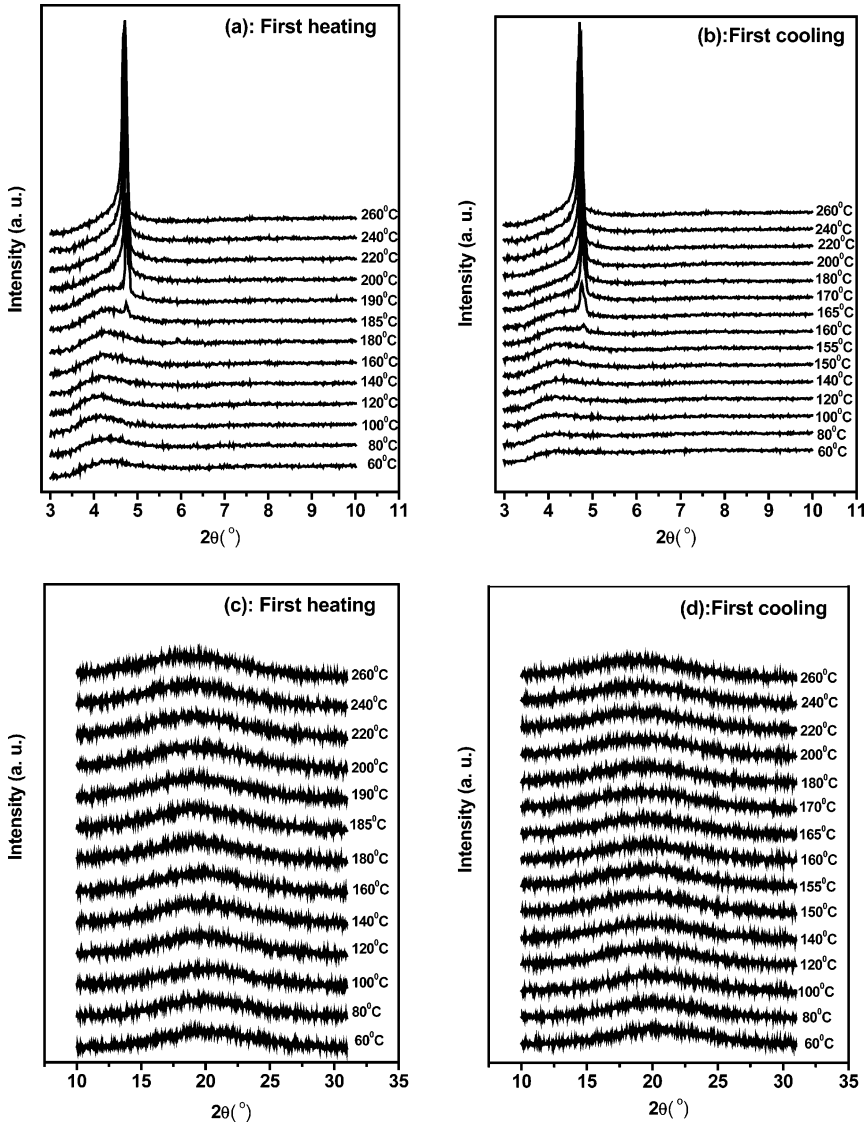

Figure 7. Powder WAXD patterns in the low 2θ angle region of sample P-10 obtained during the first heating (a) and first cooling (b) of the as-cast film. The corresponding WAXD powder patterns in the high 2θ angle regions are shown in (c) and (d).

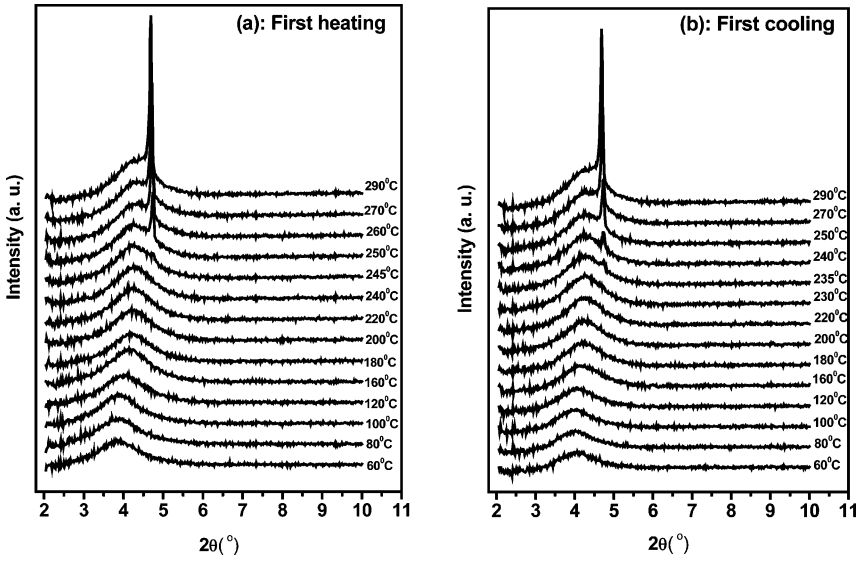

Figure 8. Powder WAXD patterns in the low 2θ angle region of sample P-4 obtained during the first heating (a) and first cooling (b) of the as-cast film.

On the cooling, the peak vanished when the temperature declined to 230 °C. Though there is not any recognizable endothermic peak in the DSC curves, this result suggests that the LC phase is formed at high temperature.

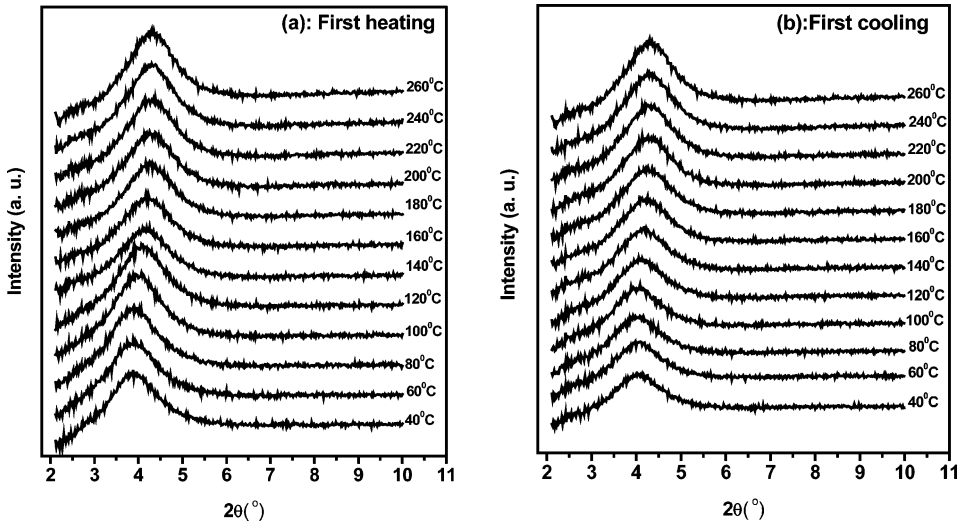

Figure 9. Powder WAXD patterns in the low 2θ angle region of sample P-1 obtained during the first heating (a) and first cooling (b) of the as-cast film.

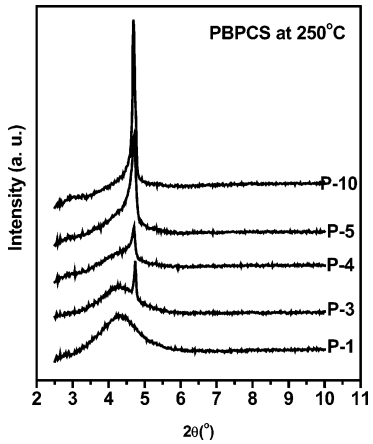

Figure 10. Set of the WAXD powder patterns at 250 °C for PBPCS with different molecular weights.

For sample P-1, the 1D WAXD patterns in Figure 9 demonstrate that the scattering halo remains broad for the entire temperature range, indicating an isotropic phase.

Figure 10 presents a set of 1D WAXD powder patterns in the low 2θ angle region for this series of PBPCS with various molecular weights obtained at 250 °C. Though the intensity of the low-angle diffraction peak increases with an increase of molecular weight as shown above, the peak occurs at almost the same 2θ angle for all the samples. This suggests that there are no major differences in the LC phase structure among the various molecular weight polymers.

The 2D WAXD patterns obtained for fibers of PBPCS are shown in Figure 11. The sample was first sheared at 210 °C and quenched rapidly to room temperature. Part a of Figure 11 shows the 2D WAXD patterns of P-10 with the X-ray incident beam perpendicular to the fiber axis. In the pattern, the fiber axis is parallel to the meridian direction. A pair of strong diffraction arcs can be found on the equator at $2\theta = 4.73°$ (d spacing of 1.87 nm), indicating that the order structure is developed parallel to fiber direction on the nanometer scale. Meanwhile, the scattering halos in the high 2θ angle are more or less concentrated on the meridians with rather broad azimuthal distributions. This indicates that only the short-range order exists along the fiber direction.

To determine the symmetry of these ordered phases, the X-ray incident beam is aligned parallel to the fiber axis, and the diffraction pattern is shown in Figure 11b. Six diffraction arcs are located at $2\theta = 4.73°$ (d spacing of 1.87 nm), which is confirmed by the corresponding azimuthal intensity profile shown in Figure 11c exhibiting six maxima with an angle of 60° between two adjacent diffraction maxima. The intensities of diffraction maxima are not identical**,** which may be caused by the defects in the sample's orientation and relaxation during cooling. Considering the similar X-ray results reported previously,[7,13,24] the supramolecular hexagonal columnar nematic phase is proposed for this sample in which the supramolecular columns, instead of the mesogen groups, possesses the nematic orientational order (Figure 12). On the basis of our low-angle WAXD results, the cylinder diameter is 2.16 nm, and the

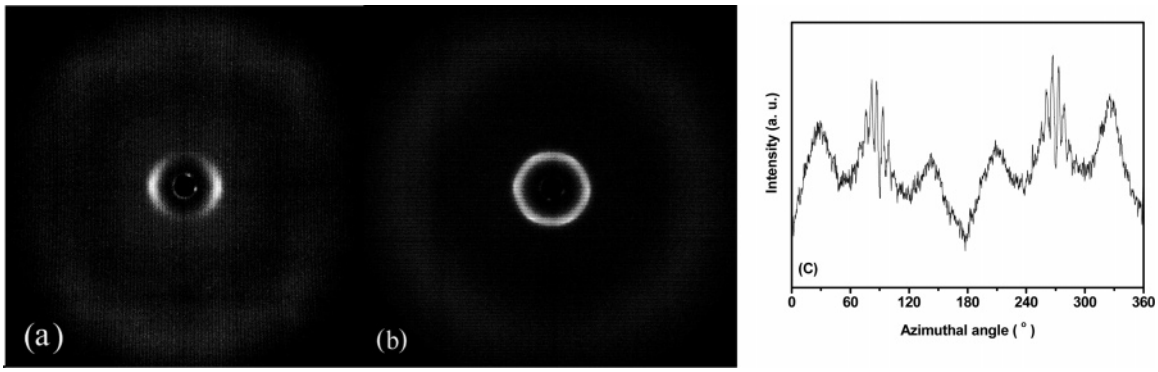

Figure 11. 2D WAXD fiber patterns of sample P-10 obtained at room temperature. The X-ray incident beam is perpendicular to the fiber axis (the meridian direction) (a) and parallel to the fiber direction (b). The azimuthal scanning data of the low 2θ angle diffraction (b) is show in (c).

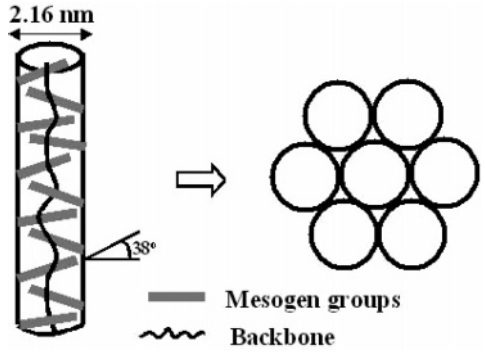

Figure 12. Schematic drawing of the chain conformation of supramolecular column (left) and hexagonal packing model (right).

molecular length of side chain is calculated around 2.75 nm. So the mesogenic groups in side chains tilts around 38°. This angle is also agreement with our precious result.[12,13]

Phase Transition Studied Using the Rheological Technique. To confirm the unusual phase transition and obtain information about the nature of various phases indicated by DSC, optical, and X-ray investigation, rheological measurements were conducted. After the rheological measurements were completed, molecular weights of the sample were checked by GPC and found to be the same as before the experiments, which indicates that no significant degradation occurred during the measurements.

The temperature dependence of viscoelastic properties from a typical heating and cooling cycle for sample P-7 is provided in parts a and b of Figure 13, respectively; the sample was loaded into the instrument at 150 °C and then cooled to 90 °C. Rheological data were then recorded at a rate of 5 °C/min. The transition temperatures evaluated by DSC at the same rates are also shown in Figure 13. It is surprising that a dramatic increase in the modulus and viscosity is observed at about 190 °C, followed by a slight increase at higher temperature. This clearly indicated a phase transition. The low viscosity of isotropic phase excludes any known optically isotropic cubic phases which are highly viscous.[25] The storage modulus is significantly greater than the loss modulus when the temperature beyond 190 °C. On the cooling cycle, the modulus decreases gradually with decreasing temperature and gets a minimal value at about 165 °C. An offset of about 20 °C is observed as compared with the temperature at the heating run.

To characterize the properties of the samples in the isotropic phase and in the LC phase, frequency sweeps (0.1−100 rad/s) for various states of the samples were performed at 170 and 220 °C, respectively (Figure 14). The data recorded at 170 °C indicate properties similar to those of the high molecular weight amorphous polymers having long side groups.[26] At the low-frequency region, the viscoelastic response of the polymer becomes liquidlike with low-frequency slopes approaching Newtonian behavior ($G' \sim \omega^2$, $G'' \sim \omega$) characteristic for the terminal flow range, which is very similar to those usually observed for flexible homopolymers in the molten state or LC polymer at isotropic state.[27,28] From a rheological point of view, there is no evidence of liquid crystallinity in this temperature region.[29] The narrow terminal relaxation is probably caused by the narrow molecular weight distribution of the polymer. However, different properties are exhibited in the LC state. The data recorded at 220 °C show highly shear thinning behavior for the complex viscosity, with the storage modulus greater than the loss modulus with both moduli essentially independent of frequency. Pluta et al.[30] studied the viscoelastic behavior of poly(oxybisdimethylsilylene) which exhibits a hexagonal nematic

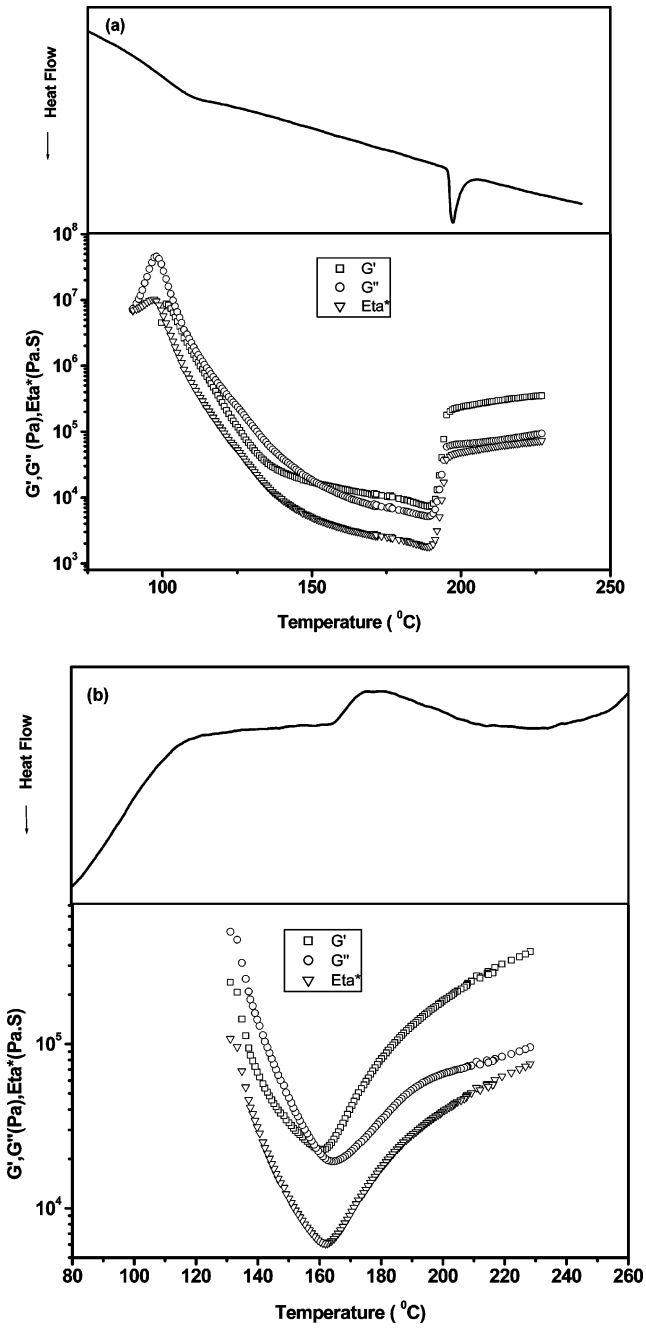

Figure 13. Heat flow (top) and magnitude of the dynamic moduli and complex viscosity (bottom) obtained during heating cycle (a) and cooling cycle (b) in DSC and rheology. Sample was loaded at 150 °C and measured with $\omega = 5$ rad/s, with a strain of 5%. The heating and cooling rate is 5 °C/min.

phase with columnar packing of extend backbones. Similar to our result, a terminal region was observed in the isotropic phase. In the mesophase state, it was observed that the dependencies of G' and G'' vs frequency were ω^{α}, where $\alpha \approx 0.8$ for both G' and G'', which was characteristic of a system with a broad relaxation time distribution vs the frequency range considered. In this case, the dependencies of G' and G'' vs frequency are weaker. It is interesting to note that the feature of viscoelastic properties of the polymer at 220 °C is similar to block copolymer possessing a hexagonal phase.[31] This suggests that it is reasonable to take the LC phase of PBPCS as hexagonal columnar nematic phase in which the single molecule acts as a rigid unit.[13] The dynamic mechanical measurements have shown that the LC phase at high temperature resembles a viscoelastic solid,

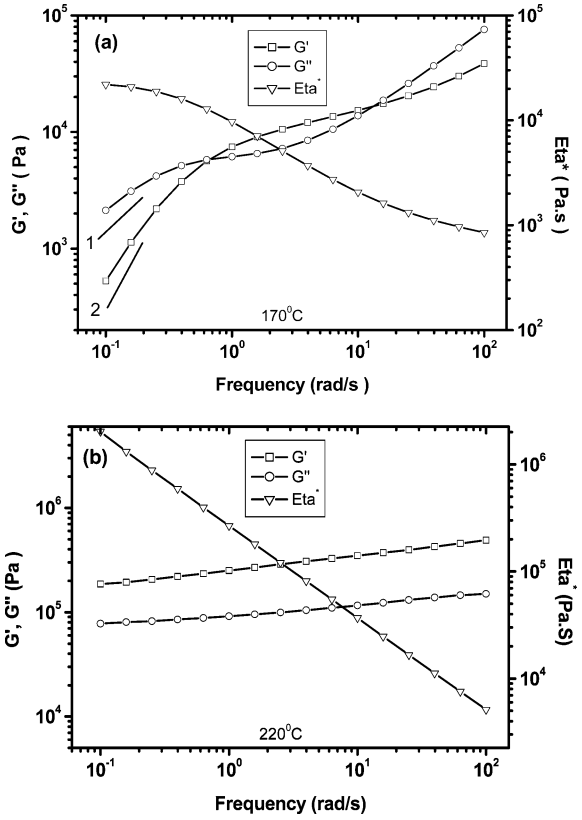

Figure 14. Magnitude of the storage modulus, loss modulus, and complex viscosity vs frequency at 170 (a) and 220 °C (b). Lines with slopes of 1 and 2 are shown to guide eyes.

while a reversible transition to a viscoelastic liquid is observed at low temperature with lower dynamic modulus and complex viscosities than those of the LC phase. The results seem to be contrary to the typical behavior of LC polymers which usually exhibit lower viscosity in LC state than that in isotropic phase.[30] This is also in contrast to conventional polymers the viscosity of which decreases with an increase of temperature.[32] However, Papkov et al.[8] studied unusual phase behavior of some poly(dialkoxyphosphazenes). In the mesomorphic state, the studied polymer is a semisolid substance. In the amorphous state, it is the optically isotropic rubberlike substance. In addition, Watanabe et al.[33] identified a columnar hexagonal liquid crystalline phase in poly(γ-octadecyl L-glutamate). This phase appears in a higher temperature than the cholesteric phase. One of the structural properties of this new phase is high viscosity. It is worth mentioning that those liquid crystalline columnar phases are not formed by conventional mesogenic groups.

Phase Diagram. According to the results of thermal behavior and X-ray scattering investigation, the phase diagram is constructed in Figure 15. It is obviously useful for the consideration of the influence of the molecular weight on the phase behavior of the PBPCS.

In the diagram, the glass temperatures are referred to the temperature of the DSC curves during the second heating scan. The temperatures of the isotropic phase to LC phase transition for high molecular weight are determined from endothermal temperature of DSC trances. For sample P-3 and P-4, the transition temperatures are based on the result of the POM observation (Table 1). The LC phase boundary is determined by X-ray scattering experiment. The degradation temperatures are outlined by a dash line as 300 °C, which is the onset degradation temperature.

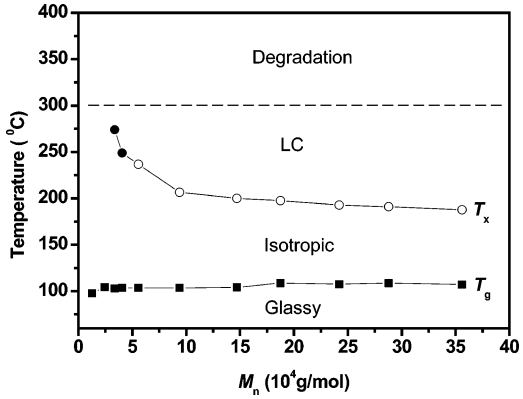

Figure 15. Phase diagram of PBPCS at second heating scan, 10 °C/min: (square) glass transition temperature and (circle) phase transition obtained by DSC; (filled circle) phase transition based on the POM observation.

The phase diagram in Figure 15 demonstrates that the phase behaviors of the PBPCS depend on the molecular weights. For PBPCS with $M_n \leq 2.42 \times 10^4$ (P-1 and P-2), there is only an isotropic phase after the glass transition temperature. With an increase of the molecular weight, the polymer enters into the LC phase from the isotropic phase. The LC phase remains until degradation. The transition temperature of the isotropic phase to the LC phase decreases with the further increasing of the molecular weight.

The existence of the isotropic−LC phase transition may be explained by the self-compacting chain model proposed by Meille et al.[34] for the mesomorphic phase of flexible polymers. For polymers having numerous, regularly spaced side groups that are often chemically different from the main chain, the key factor to stabilize mesophase is that the polymer may attain a larger entropy in the LC state over the isotropic state. The flexible backbone may become quite rigid as a consequence of their self-compacting elastic nature. Consistent to the absence of specific interchain interactions, this mesophase exhibits hexagonal packing.

For this system, the Gibbs free energy change (ΔG) from the isotropic to LC phase can be written as $\Delta G = \Delta H - T\Delta S = (H_{LC} - H_i) - T_x(S_{LC} - S_i)$. At the T_x, $\Delta G = 0$, so the enthalpy change (ΔH) at the T_x is equal to the entropy changes ($\Delta S = S_{LC} - S_i$) times T_x. When $\Delta H > 0$ for this case (Table 1), this transition is regarded as an endothermic process, where $\Delta S > 0$. This implies that the entropy in LC state is greater than that in isotropic state. The LC phase is formed by the driving force of the entropy. The heating/cooling rate dependence of the reversible phase transition for PBPCS is quite different from conventional LC polymers in which the transitions of LC polymer occur reversibly close to equilibrium and are only weakly supercooling dependent.[30] This difference can be understood when one considers that for the formation of the columnar phase of PBPCS a global change of the whole molecule from the coiled to at least partial extended conformation is required. The rigid chain conformation is supported by a higher modulus and a broader relaxation time in LC state than those in isotropic state. In addition, hexagonal packing is observed by the 2D WAXD fiber pattern, which accounts for the whole molecule acting as a rigid unit.

The presence of the isotropic phase at lower temperature before the LC phase shows a strong analogy with the well-known reentrant isotropic. According to our best knowledge, there are few reports that such a reentrant isotropic phase has been found in the thermotropic LC polymer system. However,

it should be noted that the reentrant phase has been already reported in large disklike molecules[25,35,36] and oligomers.[37] It was suggested that the conformation disordering of aliphatic tails offsets the positional ordering during phase transition. The fact that LC phase appears in a higher temperature than isotropic phase provides a helpful insight into the origin of MJLCPs and may be useful to understand the reentrant phase.

Conclusions

A series of high molecular weight PBPCS with narrow polydispersity were synthesized by ATRP. Kinetic study shows that the polymerization is under good control. For PBPCS with $M_n \geq 3.36 \times 10^4$, studies by DSC, POM, and WAXD show phase transition from isotropic to LC phase, and the LC phase formed at higher temperature disappeared upon subsequent cooling. The PBPCS samples with $M_n \leq 2.42 \times 10^4$ are isotropic. Using the 2D WAXD pattern, the phase structure of the PBPCS at higher temperature is assigned as hexagonal columnar nematic phase in which the whole molecular chain is a unit. The formation of extended chain is indicated by the heating and cooling rates dependence of the transition temperature and the linear relationship between transition temperature and reciprocal molecular weight. The phase transition is also detected by rheological measurement that shows the increasing dynamic moduli and complex viscosity. The frequency sweep experiments exhibit a terminal region in the isotropic phase (properties of a flexible polymer). In LC phase, the complex viscosity of polymer exhibits persistent shear thinning behavior, and the moduli are almost independent of the frequency with the storage modulus (G') greater than loss modulus (G'') over the investigated frequency range. On the basis of the above observation, phase diagrams are constructed depending on the molecular weight.

The LC phase is proposed to form by the driving force of the entropy, and the whole molecular motion is involved in the formation of the LC phase. Despite the higher positional ordering, the polymer has a larger entropy in the LC state than in the isotropic state.

Acknowledgment. The authors are grateful for financial support from the National Natural Science Foundation of China (Grant 20134010) and the Science Research Fund of the Chinese Ministry of Education (Grant 01001, 104005). The authors are indebted to Prof. Christopher Y. Li of Drexel University for helpful discussions about the manuscript.

References and Notes

(1) Demus, D.; Goodby, J.; Gray, G. W.; Spiess, H. W.; Vill, V. *Handbook of Liquid Crystals*; Wiley-VCH: Weinheim, 1998; Vol. 1, Chapter II, p 17.
(2) Finklemann, H.; Wendorff, H. J. Structure of Nematic Side Chain Polymers. In *Polymeric Liquid Crystals*; Blumstein, A., Ed.; Plenum Press: New York, 1985; p 295.
(3) Zhou, Q. F.; Li, H. M.; Feng, X. D. *Macromolecules* **1987**, *20*, 233.
(4) Zhou, Q. F.; Zhu, X. L.; Wen, Z. Q. *Macromolecules* **1989**, *22*, 491.
(5) Zhang, D.; Liu, Y.; Wan, X.; Zhou, Q. F. *Macromolecules* **1999**, *32*, 4494.
(6) Tu, H.; Wan, X.; Liu, Y.; Chen, X.; Zhang, D.; Zhou, Q. F.; Shen, Z.; Ge, J. J.; Jin, S.; Cheng, S. Z. D. *Macromolecules* **2000**, *33*, 6315.
(7) Yin, X.-Y.; Ye, C.; Ma, X.; Chen, E.-Q.; Qi, X.-Y.; Duan, X.-F.; Wan, X.-H.; Cheng, S. Z. D.; Zhou, Q.-F. *J. Am. Chem. Soc.* **2003**, *125*, 6854.
(8) Papkov, V. B.; Zhukov, V. P.; Tsvankin, D. J.; Tur, D. R. *Macromolecules* **1992**, *25*, 2033.
(9) Molenberg, A.; Moller, M.; Sautter, E. *Prog. Polym. Sci.* **1997**, *22*, 1133.
(10) Turetskii, A.; Out, G. J. J.; Klok, H.-A.; Moller, M. *Polymer* **1995**, *36*, 1303.
(11) Out, G. J. J.; Turetskii, A.; Moller, M.; Oelfin, D. *Macromolecules* **1994**, *27*, 3310.
(12) Li, C. Y.; Tenneti, K. K.; Zhang, D.; Zhang, H.; Wan, X.; Chen, E.-Q.; Zhou, Q.-F.; Carlos, A.-O.; Igos, S.; Hsiao, B. S. *Macromolecules* **2004**, *37*, 2854.
(13) Ye, C.; Zhang, H.-L.; Huang, Y.; Chen, E.-Q.; Lu, Y.; Shen, D.; Wan, X.-H.; Shen, Z.; Cheng, S. Z. D.; Zhou, Q.-F. *Macromolecules* **2004**, *37*, 7188.
(14) Zhang, D.; Liu, Y.; Wan, X.; Zhou, Q. F. *Macromolecules* **1999**, *32*, 5183.
(15) Yu, Z.; Wan, X.; Tu, H.; Chen, X.; Zhou, Q. F. *Acta Polym. Sin.* **2003**, *2*, 430.
(16) Xue, L.; Agarwal, U. S.; Lemstra, P. J. *Macromolecules* **2002**, *35*, 8650.
(17) Zhang, H.; Yu, Z.; Wan, X.; Zhou, Q.-F.; Woo, E. M. *Polymer* **2002**, *43*, 2357.
(18) Matyjaszewski, K.; Davis, K.; Patten, T. E.; Wei, M. *Tetrahedron* **1997**, *53*, 15321.
(19) Matyjaszewski, K.; Xia, J. *Chem. Rev.* **2001**, *101*, 2921.
(20) Keller, A.; Cheng, S. Z. D. *Polymer* **1998**, *39*, 4461.
(21) Chien, W.; Wunderlich, B. *Macromol. Chem. Phys.* **1999**, *200*, 283.
(22) Xu, G.; Hou, J.; Zhu, S.; Yang, X.; Xu, M.; Zhou, Q. F. *Polymer* **1994**, *35*, 5441.
(23) Molenberg, A.; Moller, M. *Macromolecules* **1997**, *30*, 8332.
(24) Pragliola, S.; Ober, C. K.; Mather, P. T.; Jeon, H. G. *Macromol. Chem. Phys.* **1999**, *200*, 2338.
(25) Pietrasik, U.; Szydłowska, J.; Krówczyñski, A. *Chem. Mater.* **2004**, *16*, 1485.
(26) Ferry, J. D. *Viscoelastic Properties of Polymers*; John Wiley & Sons: New York, 1980; Chapter 2.
(27) Kim, S. S.; Han, C. D. *Macromolecules* **1993**, *26*, 6633.
(28) Vlassopoulos, D.; Fytas, G.; Loppinet, B.; Isel, F.; Lutz, P.; Benoit, H. *Macromolecules* **2000**, *33*, 5960.
(29) Chang, S.; Han, C. D. *Macromolecules* **1997**, *30*, 2021.
(30) Pluta, M.; Pakula, T. *Macromol. Chem. Phys.* **1995**, *196*, 1607.
(31) Floudas, G.; Ulrich, R.; Wiesner, U. *J. Chem. Phys.* **1999**, *110*, 652.
(32) Ferry, J. D. *Viscoelastic Properties of Polymers*; John Wiley & Sons: New York, 1980; Chapter 11.
(33) Watanabe, J.; Takashina, Y. *Macromolecules* **1991**, *24*, 3423.
(34) Allegra, G.; Meille, S. V. *Macromolecules* **2004**, *37*, 3487.
(35) Pietrasik, U.; Szydłowska, J.; Krówczyñski, A.; Pociecha, D.; Górecka, E.; Guillon, D. *J. Am. Chem. Soc.* **2002**, *124*, 8884.
(36) Warmerdam, T.; Frenkel, D.; Zijlstra, R. J. J. *Liq. Cryst.* **1988**, *3*, 149.
(37) Percec, V.; Lee, M.; Heck, J.; Blackwell, H. E.; Ungar, G.; Alvarez-Castillo, A. *J. Mater. Chem.* **1992**, *2*, 931.

MA0514370